

# A fixed-stress type splitting method for nonlinear poroelasticity

Johannes Kraus<sup>1,1†</sup>, Kundan Kumar<sup>2,2†</sup>, Maria Lymbery<sup>3,3†</sup>,  
Florin A. Radu<sup>4,2\*†</sup>

<sup>1</sup>Faculty of Mathematics, University of Duisburg-Essen,  
Thea-Leymann-Straße 9, Essen, 45127, Germany.

<sup>2\*</sup>Center for Modeling of Coupled Subsurface Dynamics, Department of  
Mathematics, University of Bergen, Allégaten 41, Bergen, 5020, Norway.

<sup>3</sup>Institute for Artificial Intelligence in Medicine, University Hospital  
Essen, Girardetstraße 2, Essen, 45131, Germany.

\*Corresponding author(s). E-mail(s): [Florin.Radu@uib.no](mailto:Florin.Radu@uib.no);

Contributing authors: [johannes.kraus@uni-due.de](mailto:johannes.kraus@uni-due.de);

[Kundan.Kumar@uib.no](mailto:Kundan.Kumar@uib.no); [mariadimitrova.lymbery@uk-essen.de](mailto:mariadimitrova.lymbery@uk-essen.de);

†These authors contributed equally to this work.

## Abstract

In this paper we consider a nonlinear poroelasticity model that describes the quasi-static mechanical behaviour of a fluid-saturated porous medium whose permeability depends on the divergence of the displacement. Such nonlinear models are typically used to study biological structures like tissues, organs, cartilage and bones, which are known for a nonlinear dependence of their permeability/hydraulic conductivity on solid dilation.

We formulate (extend to the present situation) one of the most popular splitting schemes, namely the fixed-stress split method for the iterative solution of the coupled problem. The method is proven to converge linearly for sufficiently small time steps under standard assumptions. The error contraction factor then is strictly less than one, independent of the Lamé parameters, Biot and storage coefficients if the hydraulic conductivity is a strictly positive, bounded and Lipschitz-continuous function.

**Keywords:** nonlinear Biot model, soft-material poromechanics, fixed-stress splitting, convergence analysis, parameter robustness

# 1 Introduction

Coupling of flow and mechanical deformations in a porous medium, referred as poroelasticity, is relevant to several applications. These include subsurface deformations resulting from hydrocarbon recovery [1, 2] or anthropogenically induced seismic events due to geothermal stimulations [3]. In biological context, there are several examples where such a coupling is needed. For example, this is used to model the interaction between the fluid flow within the bone’s microstructure due to interstitial fluid and the mechanical deformation of the bone [4]. Similarly, the tumor growth and angiogenesis involves the interaction of solid tumor tissue, interstitial fluid flow, and angiogenesis [5]. Cartilage mechanics [6], biomechanics of soft tissues [7], brain tissues [8, 9] are other examples where the coupling of fluid flow and the deformation of solid matrix needs to be taken into account.

This paper concerns the numerical solution of the coupled flow and mechanical deformation in the context of poroelasticity. The Biot equations are the most common approach of modelling poroelasticity. In a quasi-static model they comprise a set of partial differential equations describing the flow and displacement using the physical laws of mass and momentum conservation, see Section 2.1 for the model equations. Together with linear constitutive models, the mechanical deformations are captured by an elliptic (linear elasticity) equation for the displacement and the fluid pressure is described by a parabolic equation for the evolution of the pressure. The coupling terms quantify the deformation and stress fields due to changes in the fluid pressure in addition to taking into account the changes in porosity due to mechanical deformations. Starting with the pioneering works of Terzaghi [10] and Biot [11], it was used to model the consolidation of soils [11, 12]. A comprehensive discussion of the theory of poromechanics can be found in [13]. The standard reference for the well-posedness theory for the Biot model is [14] and for more recent extensions, we refer to [15]. The quasi-static Biot model can be regarded as the singular limit of the fully dynamic Biot-Allard problem [16] after neglecting the acceleration of solid in the mechanics part.

In this work, we consider the case when the hydraulic conductivity  $K$  changes due to the evolving stress conditions, that is, upon the dilatation (local volume change),  $\text{div } \mathbf{u}$ , i.e.,  $K = K(\text{div } \mathbf{u})$ . The ease with which a fluid flows through the solid skeleton of porous media is characterized by the hydraulic conductivity tensor. It is a function of porosity and tortuosity (a measure of geometric complexity of the porous medium, see Karmen Kozeny relationships). Changes in porosity due to mechanical deformations are captured using the term  $\text{div } \mathbf{u}$ . Accordingly, the hydraulic conductivity is a function of  $\text{div } \mathbf{u}$ . Such a stress dependent permeability model was introduced first in [17] to describe poroelasticity effects in the paper production process. Same type of model is used to account for stress sensitive reservoirs in petroleum related applications [18, 19]. Mathematically, these extended Biot’s models have been studied in [20–23], where the authors have proved existence and uniqueness of solutions and developed the numerical approximations and their analysis. A comprehensive study of a nonlinear Biot model including the stress dependent permeability case and variations of boundary conditions can be found in [24]. For a recent work developing further the theory of nonlinear

single phase poroelasticity, we refer to [25]. Numerically, extensions of single phase nonlinear Biot models have been treated in [26–28].

To solve the Biot model numerically, there are two main categories of schemes: fully implicit and fully explicit. The fully implicit coupling approach considers fluid variables such as pressure and kinematic variable displacement as unknowns at each time step and linearizes the fully coupled system to obtain the Jacobian. This approach allows one to take larger time steps and provides more stability. However, there are some important disadvantages. First, the coupled linear system is difficult to solve, especially in multiphase flows where the operator of the geomechanics noticeably differs from that of the flow problem. Second, a fully coupled system may lose some flexibility, for instance, it does not permit the use of large time steps for the geomechanical response compared to the flow time step (this may be exploited to develop multirate schemes [29, 30]). Finally, the implementation of a fully implicit approach is more difficult compared to individual equations. In contrast to the implicit approach, an explicit coupling approach allows one to take the output from the mechanics (e.g., displacement) and use it as an input for the flow problem. This is simpler to implement and also allows more flexibility, for example in choosing time steps for individual equations separately. However, performing a naive explicit decoupling leads to unstable schemes or at best conditionally stable schemes.

An elegant way to combine the advantages of the above two broad approaches is to consider an iterative scheme. In this, at each step in time, the flow problem is solved followed by the mechanics problem using the pressure from the first step. The procedure is repeated until the desired convergence is reached. Since we treat the equations separately, both the ease of implementation and flexibility are retained. However, to ensure stability and robustness, the design of an iterative scheme demands careful considerations. For the fully-coupled problems, iterative methods can be used to construct efficient preconditioning techniques for the arising algebraic systems, the investigation of which is a matter of active ongoing scientific research, (see, e.g., [31–34]) including the recently developed parameter-robust methods in [35–39]).

Two main iterative coupling schemes to solve the flow problem coupled with geomechanics in an iteratively sequential manner are the fixed-stress split and the undrained split schemes [31, 38, 40] (see [41] for a variational derivation for these iterative schemes). In the fixed-stress split iterative scheme [16, 42], a constant volumetric mean total stress is assumed during the flow solve, whereas in the undrained split scheme [43, 44], a constant fluid mass is assumed during the mechanics solve. In the linear Biot case, both schemes were shown to be convergent in [16, 45, 46] and [44]. Fixed stress splitting is preferred in practice because of its robustness and efficiency. In this work we focus on the extension of fixed stress split scheme to our nonlinear setting. Our main contribution is in the convergence analysis of the fixed stress splitting scheme for the aforementioned nonlinear Biot model. The fixed stress splitting scheme introduces a stabilization of the flow equation and then iterates with the elasticity equation. This stabilization amounts to adding a diagonal term to the pressure matrix block. One key question is the amount of stabilization that should be added, which will be addressed in the proof of convergence of the scheme. Moreover, our analysis uses solution variables in their natural energy norms in contrast to the approaches in

[16, 46]. Though we treat here the fixed stress splitting scheme, the idea of the proof extends to the other types as well with necessary alterations.

The paper is organized as follows: Section 2.1 introduces the nonlinear Biot equations. The fixed-stress splitting scheme is given in Section 2.2. The convergence analysis is carried out in Section 3 and the main result is stated in Section 3.2. The numerical examples including convergence studies for different choices for  $K(\operatorname{div} \mathbf{u})$  are in Section 4 followed by conclusions in Section 5.

## 2 Problem formulation and splitting scheme

In this section, we present a nonlinear poroelasticity model that generalizes the classical quasi-static Biot's model of consolidation by introducing a general (nonlinear) dependency of the hydraulic conductivity, or, equivalently, porosity and/or permeability, on solid dilation, i.e., on the divergence of the displacement field. We further extend a popular splitting scheme for this nonlinear model, namely, the fixed-stress split method that can be used to solve the coupled problem iteratively by solving in each iterations step one mechanics and one flow equation separately.

### 2.1 A nonlinear poroelasticity model

We consider the following nonlinear poroelasticity problem in two-field formulation. Let  $\Omega$  be a bounded Lipschitz domain in  $\mathbb{R}^d$ ,  $d = 2, 3$ . Then the solid displacement  $\mathbf{u}$  and fluid pressure  $p$  are sought as the solution of the differential-algebraic system

$$-\operatorname{div} \boldsymbol{\sigma} + \alpha \nabla p = \mathbf{f} \quad \text{in } \Omega \times (0, T), \quad (1a)$$

$$\frac{\partial}{\partial t} (\alpha \operatorname{div} \mathbf{u} + Sp) - \operatorname{div} (K(\operatorname{div} \mathbf{u}) \nabla p) = g \quad \text{in } \Omega \times (0, T), \quad (1b)$$

which couples one elliptic partial differential equation (PDE), stating the momentum balance, to one parabolic PDE, stating the mass balance. Here  $\boldsymbol{\sigma} = 2\mu\boldsymbol{\epsilon}(\mathbf{u}) + \lambda \operatorname{div} \mathbf{u} \mathbf{I}$  denotes the effective stress where  $\boldsymbol{\epsilon}(\mathbf{u}) = \frac{1}{2}(\nabla \mathbf{u} + (\nabla \mathbf{u})^T)$  is the strain tensor and  $\lambda$  and  $\mu$  are given Lamé parameters. The remaining model parameters are the Biot-Willis coefficient  $\alpha$ , the constrained storage coefficient  $S$ , and the hydraulic conductivity  $K$ , which itself is defined in terms of the intrinsic permeability  $\mathbb{K}$ , the fluid density  $\rho$  and viscosity  $\eta$  (and the gravitational constant  $c_g$ ) via the relation  $K = \mathbb{K}\rho c_g/\eta$ .

Moreover, we want to make the following assumption.

**Assumption 1.** *We assume that the hydraulic conductivity  $K : \mathbb{R} \mapsto \mathbb{R}$  is differentiable, strictly positive, bounded from above, and Lipschitz continuous with a Lipschitz constant  $K_L$ , i.e., the function  $K$  satisfies the conditions*

$$K \in C^1(\mathbb{R}), \quad (2a)$$

$$0 < K_0 \leq K(z) \text{ for all } z \in \mathbb{R}, \quad (2b)$$

$$K(z) \leq K_1 < \infty \text{ for all } z \in \mathbb{R}, \quad (2c)$$

$$|K(z_1) - K(z_2)| \leq K_L |z_1 - z_2| \text{ for all } z_1, z_2 \in \mathbb{R}. \quad (2d)$$

Then, under Assumption 1 and imposing proper boundary and initial conditions, the system (1) has a unique solution. For instance, such conditions are given by

$$\begin{aligned}
p(\mathbf{x}, t) &= p_D(\mathbf{x}, t), & \mathbf{x} \in \Gamma_{p,D}, & \quad t > 0, \\
\frac{\partial p(\mathbf{x}, t)}{\partial \mathbf{n}} &= q_N(\mathbf{x}, t), & \mathbf{x} \in \Gamma_{p,N}, & \quad t > 0, \\
\mathbf{u}(\mathbf{x}, t) &= \mathbf{u}_D(\mathbf{x}, t), & \mathbf{x} \in \Gamma_{\mathbf{u},D}, & \quad t > 0, \\
(\boldsymbol{\sigma}(\mathbf{x}, t) - \alpha p \mathbf{I}) \mathbf{n}(\mathbf{x}) &= \mathbf{v}_N(\mathbf{x}, t), & \mathbf{x} \in \Gamma_{\mathbf{u},N}, & \quad t > 0, \\
p(\mathbf{x}, 0) &= p_0(\mathbf{x}), & \mathbf{x} \in \Omega, & \\
\mathbf{u}(\mathbf{x}, 0) &= \mathbf{u}_0(\mathbf{x}), & \mathbf{x} \in \Omega, &
\end{aligned}$$

where  $\Gamma_{p,D} \cap \Gamma_{p,N} = \emptyset$ ,  $\bar{\Gamma}_{p,D} \cup \bar{\Gamma}_{p,N} = \Gamma = \partial\Omega$ ,  $\Gamma_{\mathbf{u},D} \cap \Gamma_{\mathbf{u},N} = \emptyset$  and  $\bar{\Gamma}_{\mathbf{u},D} \cup \bar{\Gamma}_{\mathbf{u},N} = \Gamma$  are fulfilled.

We divide (1a) by  $2\mu$  and (1b) by  $\alpha$  and introduce the new variable  $\tilde{p} = \frac{\alpha}{(2\mu)}p$  and obtain the equivalent system

$$-\operatorname{div}(\boldsymbol{\epsilon}(\mathbf{u}) + \tilde{\lambda} \operatorname{div} \mathbf{u} \mathbf{I}) + \nabla \tilde{p} = \tilde{\mathbf{f}} \quad \text{in } \Omega \times (0, T), \quad (3a)$$

$$\frac{\partial}{\partial t} (\operatorname{div} \mathbf{u} + \tilde{S} \tilde{p}) - \operatorname{div}(\tilde{K}(\operatorname{div} \mathbf{u}) \nabla \tilde{p}) = \tilde{g} \quad \text{in } \Omega \times (0, T), \quad (3b)$$

for the scaled parameters  $\tilde{\lambda} = \lambda/(2\mu)$ ,  $\tilde{S} = \frac{2\mu S}{\alpha^2}$ , scaled right-hand sides  $\tilde{\mathbf{f}} = \mathbf{f}/(2\mu)$ ,  $\tilde{g} = g/\alpha$ , and the scaled function  $\tilde{K}(\operatorname{div} \mathbf{u}) = \frac{2\mu}{\alpha^2} K(\operatorname{div} \mathbf{u})$ , the latter satisfying Assumption 1 if and only if  $K$  does.

Next, on a given subdivision  $0 = t_0 < t_1 < \dots < t_{n-1} < t_n < \dots < t_{N-1} < t_N = T$  of the time interval  $[0, T]$  into subintervals  $[t_{n-1}, t_n]$  of length  $\tau := \tau_n = t_n - t_{n-1}$ ,  $n = 1, 2, \dots, N$ , we discretize in time equation (3b) by the implicit Euler method. Since in what follows we consider only a single time-step, for convenience, we denote the quantities of interest at time  $t_n$  by  $\mathbf{u} := \mathbf{u}_n = \mathbf{u}(\mathbf{x}, t_n)$  and  $p := \tilde{p}_n = p(\mathbf{x}, t_n)$ , and use the short notation  $\mathbf{f} := \mathbf{f}(\mathbf{x}, t_n)$  and  $g = \tau \tilde{g}(\mathbf{x}, t_n) + \operatorname{div} \mathbf{u}_{n-1} + \tilde{S} p_{n-1}$  for the right-hand sides in the implicit Euler time-step equations, where we assume that  $\mathbf{u}_{n-1}$  and  $\tilde{p}_{n-1}$  are known from initial conditions or have already been computed. Moreover, from now on, we will also skip the tilde symbol again with the scaled parameters in (3), including the scaled hydraulic conductivity.

The variational form of the time-step equations can then be expressed as: Find  $(\mathbf{u}, p) \in \mathbf{U} \times P$  such that

$$(\boldsymbol{\epsilon}(\mathbf{u}), \boldsymbol{\epsilon}(\mathbf{w})) + \lambda(\operatorname{div} \mathbf{u}, \operatorname{div} \mathbf{w}) - (p, \operatorname{div} \mathbf{w}) = (\mathbf{f}, \mathbf{w}), \quad \forall \mathbf{w} \in \mathbf{U}, \quad (4a)$$

$$(\operatorname{div} \mathbf{u}, q) - \tau(\operatorname{div} K(\operatorname{div} \mathbf{u}) \nabla p, q) + S(p, q) = (g, q), \quad \forall q \in P, \quad (4b)$$

where the choice of the spaces  $\mathbf{U}$  and  $P$  depends on the boundary conditions, e.g.,  $\mathbf{U} = \mathbf{H}_0^1(\Omega)$  and  $P = L_0^2(\Omega)$  for  $\Gamma_{\mathbf{u},D} = \Gamma_{p,N} = \Gamma$ . System (4) will be our object of interest in the remainder of this paper.

**Remark 1.** *When the hydraulic conductivity  $K$  is constant, the model equations become linear. They are a coupled system of an elliptic equation for the displacement*

$\mathbf{u}$  and a parabolic equation for  $p$ . The linear problem has been intensively investigated including the existence and uniqueness of a solution, and its numerical approximations.

## 2.2 Fixed-stress splitting method

The fixed-stress splitting method can be used to solve iteratively system (4), i.e. for approximating its solution  $(\mathbf{u}, p) = (\mathbf{u}_n, p_n)$  at time  $t = t_n$  starting with an arbitrary initial guess  $(\mathbf{u}^0, p^0)$  thereby using an already known approximation of  $(\mathbf{u}_{n-1}, p_{n-1})$ , which can be computed by the same method. In order to avoid confusion with time-stepping, we will use superscripts for the iteration counters in the studied splitting scheme. Algorithm 1 below describes this iterative process that consists of computing alternately an update  $p^{i+1}$  from a stabilized mass-balance equation, assuming a constant volumetric mean stress  $\lambda \operatorname{div} \mathbf{u}^i - L \lambda \alpha^{-1} p^i$ , where  $L$  is a free to be chosen stabilization parameter, i.e., solving equation (5) and an update  $\mathbf{u}^{i+1}$  arising from solution of the momentum balance equation (6). The process is continued until a certain convergence criterion is satisfied.

---

### Algorithm 1 Fixed-stress splitting method in variational form

---

Execute alternately steps (a) and (b) until the convergence criterion is satisfied.

(a) Given  $\mathbf{u}^i$  and  $p^i$  and  $K^i := K(\operatorname{div} \mathbf{u}^i)$ , solve for  $p^{i+1}$  the equation

$$-\tau(\operatorname{div} K^i \nabla p^{i+1}, q) + S(p^{i+1}, q) + L(p^{i+1}, q) = (g, q) + L(p^i, q) - (\operatorname{div} \mathbf{u}^i, q), \quad \forall q \in P. \quad (5)$$

(b) Given  $p^{i+1}$ , solve for  $\mathbf{u}^{i+1}$  the equation

$$(\boldsymbol{\epsilon}(\mathbf{u}^{i+1}), \boldsymbol{\epsilon}(\mathbf{w})) + \lambda(\operatorname{div} \mathbf{u}^{i+1}, \operatorname{div} \mathbf{w}) = (\mathbf{f}, \mathbf{w}) + (p^{i+1}, \operatorname{div} \mathbf{w}), \quad \forall \mathbf{w} \in \mathbf{U}. \quad (6)$$


---

Note that the above algorithm is essentially the classical fixed stress method in which we use the hydraulic conductivity  $K^i$  from the previous iteration in equation (5).

**Remark 2.** *In the linear case (constant  $K$ ), the iterative splitting schemes have been extensively studied for this multiphysics problem. We refer to [47] for a first convergence analysis, then to [48] for an extension to heterogeneous flow and by using energy norms. The question of an optimal stabilization parameter  $L$  (i.e. the value of  $L$  which leads to the minimal number of iterations) was discussed in detail in [38, 49], where also the connection between the stability of the discretization and the convergence of the splitting scheme has been made.*

**Remark 3.** *The fixed-stress splitting scheme presented above can be seen as a combination between a linearization scheme, the  $L$ -scheme (see [50]) and the fixed-stress splitting scheme for linear problems. This was already previously applied for other classes of nonlinear Biot models, as e.g. in [26, 28] or for unsaturated flow in deformable porous media [51]. This type of methods are often accelerated by using the Anderson Acceleration method, see e.g. [51].*

### 3 Convergence analysis

In this section we present the convergence analysis of Algorithm 1 for the iterative solution of the nonlinear poroelasticity problem (4).

#### 3.1 Auxiliary results

In order to analyze the fixed-stress split method, i.e., prove its uniform linear convergence for an arbitrary initial guess  $(\mathbf{u}^0, p^0)$ , we define the errors associated with the approximations  $\mathbf{u}^i$  and  $p^i$  after  $i$  executions of steps (a) and (b) of Algorithm 1, i.e.,

$$\mathbf{e}_u^i := \mathbf{u}^i - \mathbf{u} \in \mathbf{U}, \quad (7a)$$

$$e_p^i := p^i - p \in P, \quad (7b)$$

where  $i = 0, 1, 2, \dots$ , and  $(\mathbf{u}, p)$  denotes the exact solution of the coupled problem (4).

Subtracting from equations (5) and (6), which are solved in the  $(i+1)$ -st iteration, the equations (4b) and (4a) results in the error equations

$$\begin{aligned} -\tau(\operatorname{div} K^i \nabla p^{i+1} - \operatorname{div} K \nabla p, q) + S(e_p^{i+1}, q) \\ + L(e_p^{i+1}, q) = L(e_p^i, q) - (\operatorname{div} \mathbf{e}_u^i, q), \quad \forall q \in P, \end{aligned} \quad (8a)$$

$$(\boldsymbol{\epsilon}(\mathbf{e}_u^{i+1}), \boldsymbol{\epsilon}(\mathbf{w})) + \lambda(\operatorname{div} \mathbf{e}_u^{i+1}, \operatorname{div} \mathbf{w}) = (e_p^{i+1}, \operatorname{div} \mathbf{w}), \quad \forall \mathbf{w} \in \mathbf{U}, \quad (8b)$$

where we have used the short notation  $K := K(\operatorname{div} \mathbf{u})$ . Now, using the test functions  $q = e_p^{i+1}$  and  $\mathbf{w} := \mathbf{e}_u^{i+1}$  in (8) and adding up the resulting equations (8a) and (8b), we obtain an error identity, which serves as the basis for our analysis, that is,

$$\begin{aligned} \|\boldsymbol{\epsilon}(\mathbf{e}_u^{i+1})\|^2 + \lambda \|\operatorname{div} \mathbf{e}_u^{i+1}\|^2 + \tau(K^i \nabla p^{i+1} - K \nabla p, \nabla e_p^{i+1}) \\ + S\|e_p^{i+1}\|^2 + L((e_p^{i+1} - e_p^i), e_p^{i+1}) = (\operatorname{div}(\mathbf{e}_u^{i+1} - \mathbf{e}_u^i), e_p^{i+1}). \end{aligned} \quad (9)$$

The following lemma provides an estimate that can be derived from (9), bounding quantities associated with the approximations after  $(i+1)$  iterations by the norm of the error  $e_p^i$ .

**Lemma 1.** *Consider the approximations  $\mathbf{u}^{i+1}$  and  $p^{i+1}$  generated via Algorithm 1 and the corresponding errors  $\mathbf{e}_u^{i+1}$  and  $e_p^{i+1}$  defined according to (7), where  $(\mathbf{u}, p)$  is the exact solutions of problem (4). Then for a stabilization parameter  $L \geq 1/(d^{-1} + \lambda) =: 1/(c_K^2 + \lambda)$  there holds the estimate*

$$\begin{aligned} \frac{1}{2} (\|\boldsymbol{\epsilon}(\mathbf{e}_u^{i+1})\|^2 + \lambda \|\operatorname{div} \mathbf{e}_u^{i+1}\|^2) + \tau(K^i \nabla p^{i+1} - K \nabla p, \nabla e_p^{i+1}) \\ + S\|e_p^{i+1}\|^2 + \frac{L}{2} \|e_p^{i+1}\|^2 \leq \frac{L}{2} \|e_p^i\|^2. \end{aligned} \quad (10)$$

*Proof.* In view of  $(e_p^{i+1} - e_p^i, e_p^{i+1}) = \frac{1}{2} (\|e_p^{i+1} - e_p^i\|^2 + \|e_p^{i+1}\|^2 - \|e_p^i\|^2)$  we can rewrite (9) in the form

$$\begin{aligned} & \|\epsilon(e_u^{i+1})\|^2 + \lambda \|\operatorname{div} e_u^{i+1}\|^2 + \tau(K^i \nabla p^{i+1} - K \nabla p, \nabla e_p^{i+1}) \\ & \quad + S \|e_p^{i+1}\|^2 + \frac{L}{2} \|e_p^{i+1}\|^2 + \frac{L}{2} \|e_p^{i+1} - e_p^i\|^2 \\ & = \frac{L}{2} \|e_p^i\|^2 + (\operatorname{div}(e_u^{i+1} - e_u^i), e_p^{i+1}). \end{aligned} \quad (11)$$

Next, for  $w = e_u^{i+1} - e_u^i$ , the error equation (8b) gives

$$(\operatorname{div}(e_u^{i+1} - e_u^i), e_p^{i+1}) = (\epsilon(e_u^{i+1}), \epsilon(e_u^{i+1} - e_u^i)) + \lambda(\operatorname{div} e_u^{i+1}, \operatorname{div}(e_u^{i+1} - e_u^i)). \quad (12)$$

Now, inserting (12) in (11), we obtain

$$\begin{aligned} & \|\epsilon(e_u^{i+1})\|^2 + \lambda \|\operatorname{div} e_u^{i+1}\|^2 + \tau(K^i \nabla p^{i+1} - K \nabla p, \nabla e_p^{i+1}) \\ & \quad + S \|e_p^{i+1}\|^2 + \frac{L}{2} \|e_p^{i+1}\|^2 + \frac{L}{2} \|e_p^{i+1} - e_p^i\|^2 \\ & = \frac{L}{2} \|e_p^i\|^2 + (\epsilon(e_u^{i+1}), \epsilon(e_u^{i+1} - e_u^i)) + \lambda(\operatorname{div} e_u^{i+1}, \operatorname{div}(e_u^{i+1} - e_u^i)) \\ & \leq \frac{L}{2} \|e_p^i\|^2 + \frac{1}{2} (\|\epsilon(e_u^{i+1})\|^2 + \lambda \|\operatorname{div} e_u^{i+1}\|^2) \\ & \quad + \frac{1}{2} (\|\epsilon(e_u^{i+1} - e_u^i)\|^2 + \lambda \|\operatorname{div}(e_u^{i+1} - e_u^i)\|^2), \end{aligned} \quad (13)$$

and, after collecting terms,

$$\begin{aligned} & \frac{1}{2} (\|\epsilon(e_u^{i+1})\|^2 + \lambda \|\operatorname{div} e_u^{i+1}\|^2) + \tau(K^i \nabla p^{i+1} - K \nabla p, \nabla e_p^{i+1}) \\ & \quad + S \|e_p^{i+1}\|^2 + \frac{L}{2} \|e_p^{i+1}\|^2 + \frac{L}{2} \|e_p^{i+1} - e_p^i\|^2 \\ & \leq \frac{L}{2} \|e_p^i\|^2 \\ & \quad + \frac{1}{2} (\|\epsilon(e_u^{i+1} - e_u^i)\|^2 + \lambda \|\operatorname{div}(e_u^{i+1} - e_u^i)\|^2). \end{aligned} \quad (14)$$

What remains to be done is to estimate the last term on the right-hand side of (14). For this purpose, we subtract the error equation (8b) for the  $i$ -th error  $e_u^i$  from that for the  $(i+1)$ -st error  $e_u^{i+1}$  and test with  $w = e_u^{i+1} - e_u^i$ , resulting in

$$\begin{aligned} \|\epsilon(e_u^{i+1} - e_u^i)\|^2 + \lambda \|\operatorname{div}(e_u^{i+1} - e_u^i)\|^2 & = (e_p^{i+1} - e_p^i, \operatorname{div}(e_u^{i+1} - e_u^i)) \\ & \leq \|e_p^{i+1} - e_p^i\| \|\operatorname{div}(e_u^{i+1} - e_u^i)\|. \end{aligned} \quad (15)$$



Moreover, using the inequality  $\|\boldsymbol{\epsilon}(\mathbf{w})\| \geq c_K \|\operatorname{div} \mathbf{w}\|$ , which is valid for all  $\mathbf{w} \in \mathbf{U}$  for  $c_K = \frac{1}{\sqrt{d}}$  where  $d$  is the space dimension, from (15) we get

$$(c_K^2 + \lambda) \|\operatorname{div}(\mathbf{e}_{\mathbf{u}}^{i+1} - \mathbf{e}_{\mathbf{u}}^i)\|^2 \leq \|e_p^{i+1} - e_p^i\| \|\operatorname{div}(\mathbf{e}_{\mathbf{u}}^{i+1} - \mathbf{e}_{\mathbf{u}}^i)\|,$$

or, equivalently,

$$\|\operatorname{div}(\mathbf{e}_{\mathbf{u}}^{i+1} - \mathbf{e}_{\mathbf{u}}^i)\| \leq \frac{1}{c_K^2 + \lambda} \|e_p^{i+1} - e_p^i\|. \quad (16)$$

Now, combining (15) and (16), we find

$$\begin{aligned} \|\boldsymbol{\epsilon}(\mathbf{e}_{\mathbf{u}}^{i+1} - \mathbf{e}_{\mathbf{u}}^i)\|^2 + \lambda \|\operatorname{div}(\mathbf{e}_{\mathbf{u}}^{i+1} - \mathbf{e}_{\mathbf{u}}^i)\|^2 &\leq \frac{1}{c_K^2 + \lambda} \|e_p^{i+1} - e_p^i\|^2 \\ &\leq L \|e_p^{i+1} - e_p^i\|^2, \end{aligned} \quad (17)$$

where the last inequality holds due to the assumption  $L \geq 1/(c_K^2 + \lambda)$ . Finally, using (17) in (14) yields (10), the estimate we had to prove.  $\square$

Before we prove the main result of this paper, we present another lemma that will turn out to be useful.

**Lemma 2.** *For the errors associated with the iterates generated by Algorithm 1 there holds the estimate*

$$(\beta_s^{-2} + \lambda)^{-1} \|e_p^{i+1}\|^2 \leq \|\boldsymbol{\epsilon}(\mathbf{e}_{\mathbf{u}}^{i+1})\|^2 + \lambda \|\operatorname{div} \mathbf{e}_{\mathbf{u}}^{i+1}\|^2 \quad (18)$$

where  $\beta_s$  is the constant in the Stokes inf-sup condition

$$\inf_{q \in P} \sup_{\mathbf{w} \in \mathbf{U}} \frac{(\operatorname{div} \mathbf{w}, q)}{\|\mathbf{w}\|_1 \|q\|} \geq \beta_s. \quad (19)$$

*Proof.* As one can easily see, the Stokes inf-sup condition (19) implies that for any  $e_p^{i+1}$  there exists  $\mathbf{w}_p \in \mathbf{U}$  such that

$$\operatorname{div} \mathbf{w}_p = e_p^{i+1} \quad \text{and} \quad \|\boldsymbol{\epsilon}(\mathbf{w}_p)\| \leq \beta_s^{-1} \|e_p^{i+1}\|. \quad (20)$$

Hence, this element  $\mathbf{w}_p$  satisfies the estimate

$$\|\boldsymbol{\epsilon}(\mathbf{w}_p)\|^2 + \lambda \|\operatorname{div} \mathbf{w}_p\|^2 \leq (\beta_s^{-2} + \lambda) \|e_p^{i+1}\|^2.$$

Setting  $\mathbf{w} = \mathbf{w}_p$  in (8b) and using (20), we obtain

$$\begin{aligned} \|e_p^{i+1}\|^2 &= (\boldsymbol{\epsilon}(\mathbf{e}_{\mathbf{u}}^{i+1}), \boldsymbol{\epsilon}(\mathbf{w}_p)) + \lambda (\operatorname{div} \mathbf{e}_{\mathbf{u}}^{i+1}, \operatorname{div} \mathbf{w}_p) \\ &\leq (\|\boldsymbol{\epsilon}(\mathbf{e}_{\mathbf{u}}^{i+1})\|^2 + \lambda \|\operatorname{div} \mathbf{e}_{\mathbf{u}}^{i+1}\|^2)^{\frac{1}{2}} (\|\boldsymbol{\epsilon}(\mathbf{w}_p)\|^2 + \lambda \|\operatorname{div} \mathbf{w}_p\|^2)^{\frac{1}{2}} \\ &\leq (\|\boldsymbol{\epsilon}(\mathbf{e}_{\mathbf{u}}^{i+1})\|^2 + \lambda \|\operatorname{div} \mathbf{e}_{\mathbf{u}}^{i+1}\|^2)^{\frac{1}{2}} (\beta_s^{-2} + \lambda)^{\frac{1}{2}} \|e_p^{i+1}\| \end{aligned}$$

which shows the desired result.  $\square$

**Remark 4.** *The above method of contraction uses solution variables and their natural energy norms. This is in the same spirit as the proofs of contraction as carried out in [38, 39, 45, 49]. This is in contrast to the convergence analysis as carried out in [16, 44, 46] where the contraction is proved for composition quantities consisting of both pressure and displacement terms. For example, in case of fixed stress split scheme, a volumetric mean stress is defined by  $\sigma = \lambda \nabla \cdot \mathbf{u} - \alpha p$  and the contraction is proved on this composite quantity [16].*

### 3.2 Main result

Lemma 1 and Lemma 2 are the key ingredients to establish the uniform convergence of the fixed-stress split method under Assumption 1.

**Theorem 3.** *Consider the fixed-stress split iteration according to Algorithm 1 to approximate the exact solution  $(\mathbf{u}, p)$  of the nonlinear problem (4) in which the hydraulic conductivity  $K = K(\text{div } \mathbf{u})$  is a function of the dilation of the solid that satisfies the conditions in Assumption 1. Further, assume that  $\nabla p \in L^\infty(\Omega)$ .*

*Then the iterates  $(\mathbf{u}^i, p^i)$  converge linearly to  $(\mathbf{u}, p)$  for a sufficiently small time step  $\tau$ . In particular, the following estimates holds:*

$$\|e_p^{i+1}\| \leq \sqrt{\frac{c_0 + \frac{\tau}{4K_0} \frac{c^2}{(c_K^2 + \lambda)^2}}{c_1}} \|e_p^i\|, \quad (21)$$

$$\left( \|\epsilon(\mathbf{e}_u^{i+1})\|^2 + \lambda \|\text{div } \mathbf{e}_u^{i+1}\|^2 \right)^{\frac{1}{2}} \leq \sqrt{\frac{1}{c_K^2 + \lambda}} \|e_p^{i+1}\|, \quad (22)$$

where  $c_0 := L/2 < c_1 := L/2 + (\beta_s^{-2} + \lambda)^{-1}/2$  and  $L$  is the stabilization parameter in Algorithm 1 and  $\beta_s$  the Stokes inf-sup constant.

*Proof.* The inner product  $\tau(K^i \nabla p^{i+1} - K \nabla p, \nabla e_p^{i+1})$  in (10) can be represented as

$$\begin{aligned} \tau(K(\text{div } \mathbf{u}^i) \nabla p^{i+1} - K(\text{div } \mathbf{u}) \nabla p, \nabla e_p^{i+1}) &= \tau((K(\text{div } \mathbf{u}^i) - K(\text{div } \mathbf{u})) \nabla p, \nabla e_p^{i+1}) \\ &\quad + \tau(K(\text{div } \mathbf{u}^i) \nabla e_p^{i+1}, \nabla e_p^{i+1}) \end{aligned} \quad (23)$$

The two terms in this splitting, due to Assumption 1, can be estimated as follows:

$$\begin{aligned} \tau((K(\text{div } \mathbf{u}^i) - K(\text{div } \mathbf{u})) \nabla p, \nabla e_p^{i+1}) &\leq \tau c \|\text{div } \mathbf{e}_u^i\| \|\nabla e_p^{i+1}\| \\ &\leq \tau c \left( \frac{1}{2\delta} \|\text{div } \mathbf{e}_u^i\|^2 + \frac{\delta}{2} \|\nabla e_p^{i+1}\|^2 \right) \end{aligned} \quad (24)$$

$$\tau(K(\text{div } \mathbf{u}^i) \nabla e_p^{i+1}, \nabla e_p^{i+1}) \geq \tau K_0 \|\nabla e_p^{i+1}\|^2 \quad (25)$$

where in the first inequality in (24) we have used the boundedness of  $\nabla p$ , i.e.,  $\|\nabla p\|_{L^\infty} \leq c_\infty$  as well as the Lipschitz continuity of  $K$ , i.e.,

$$|K(\text{div } \mathbf{u}^i) - K(\text{div } \mathbf{u})| \leq K_L |\text{div } \mathbf{u}^i - \text{div } \mathbf{u}| = K_L |\text{div } \mathbf{e}_u^i|,$$

which means that we can choose  $c := c_\infty K_L$  and the positive constant  $\delta$  in the second inequality in (24) is still at our disposal. To obtain (25) we have used the strict positivity of  $K$ , see (2b).

Combining (10) and (18), we obtain

$$\frac{1}{2}(\beta_s^{-2} + \lambda)^{-1} \|e_p^{i+1}\|^2 + \tau(K^i \nabla p^{i+1} - K \nabla p, \nabla e_p^{i+1}) + S \|e_p^{i+1}\|^2 + \frac{L}{2} \|e_p^{i+1}\|^2 \leq \frac{L}{2} \|e_p^i\|^2$$

which implies

$$\frac{1}{2} \left( \frac{1}{\beta_s^{-2} + \lambda} + L \right) \|e_p^{i+1}\|^2 + \tau(K^i \nabla p^{i+1} - K \nabla p, \nabla e_p^{i+1}) \leq \frac{L}{2} \|e_p^i\|^2. \quad (26)$$

We rewrite the latter estimate as

$$c_1 \|e_p^{i+1}\|^2 + \tau(K^i \nabla p^{i+1} - K \nabla p, \nabla e_p^{i+1}) \leq c_0 \|e_p^i\|^2. \quad (27)$$

using the definitions  $0 < c_0 := L/2 < c_1 := L/2 + (\beta_s^{-2} + \lambda)^{-1}/2$ . Taking advantage of the splitting (23) and the estimates (24) and (25), from (27) we find

$$\begin{aligned} c_1 \|e_p^{i+1}\|^2 + \tau K_0 \|\nabla e_p^{i+1}\|^2 &\leq c_0 \|e_p^i\|^2 + \tau c \|\operatorname{div} \mathbf{e}_u^i\| \|\nabla e_p^{i+1}\| \\ &\leq c_0 \|e_p^i\|^2 + \tau c \frac{1}{c_K^2 + \lambda} \|e_p^i\| \|\nabla e_p^{i+1}\| \\ &\leq c_0 \|e_p^i\|^2 + \tau c \frac{1}{c_K^2 + \lambda} \left( \frac{1}{2\delta} \|e_p^i\|^2 + \frac{\delta}{2} \|\nabla e_p^{i+1}\|^2 \right). \end{aligned} \quad (28)$$

where we have also used the error equation (8b) in a similar way as in the derivation of (16).

Now, we choose  $\delta := \frac{2K_0(c_K^2 + \lambda)}{c}$ , to cancel the terms with  $\|\nabla e_p^{i+1}\|^2$  on both sides of (28) in order to obtain

$$c_1 \|e_p^{i+1}\|^2 \leq \left( c_0 + \frac{\tau}{4K_0} \frac{c^2}{(c_K^2 + \lambda)^2} \right) \|e_p^i\|^2, \quad (29)$$

the latter being equivalent to (21).

Finally, estimate (22) follows in a similar way as (17) (from the error equation (8b) by setting  $\mathbf{w} = \mathbf{e}_u^{i+1}$  and using  $\|\boldsymbol{\epsilon}(\mathbf{w})\| \geq c_K \|\operatorname{div} \mathbf{w}\|$ ).  $\square$

**Remark 5.** A simple choice for the stabilization parameter is  $L := 1/(c_K^2 + \lambda) = 1/(d^{-1} + \lambda)$ , which together with the definitions in the Theorem 3, i.e.,  $c_0 := L/2$  and  $c_1 := L/2 + (\beta_s^{-2} + \lambda)^{-1}/2$ , results in a quotient  $c_0/c_1 = 1/(1 + \frac{1+2\lambda}{2\beta_s^{-2}+2\lambda})$ . This means that for small values of  $\tau$  the theoretical bound on the  $L^2$ -error contraction factor approaches  $(1 + \frac{1+2\lambda}{2\beta_s^{-2}+2\lambda})^{-1/2}$  and for  $\lambda \rightarrow \infty$  its limit is  $1/\sqrt{2}$ , which is in accordance with the corresponding estimate for the linear problem, as presented in [52].

**Remark 6.** *The number of iterations is obviously depending on the choice of the parameter  $L$ . To find an optimal  $L$  is typically not an easy task. We refer to the work [49] for a detailed study on how to chose an optimal  $L$  for the splitting scheme for the quasi-static linear Biot model.*

## 4 Numerical results

The aim of this section is to numerically test the performance of the proposed fixed-stress Algorithm 1. To this end, we consider the following test problems of type (1) which differ only in the definition of the permeability coefficient function  $K$ , namely

- (o)  $K = K_0$ , i.e., a linear model;
- (i)  $K = K(\operatorname{div} \mathbf{u}) = K_0 + K_1(\operatorname{div} \mathbf{u})^2$ ;
- (ii)  $K = K(\operatorname{div} \mathbf{u}) = (K_0 + K_1 \operatorname{div} \mathbf{u})^2$ ;
- (iii)  $K = K(\operatorname{div} \mathbf{u}) = K_0 e^{K_1 \operatorname{div} \mathbf{u}}$ ,

where the constants  $K_0$  and  $K_1$  are specified within the description of the individual test settings.

In all computations we have used homogeneous Dirichlet boundary conditions for  $\mathbf{u}$  and homogeneous Neumann boundary conditions for  $p$ . The chosen computational domain  $\Omega$  is the L-shaped region  $\Omega = (0, 1) \times (0, 1) \setminus [0.5, 1) \times [0.5, 1)$ , which is a standard choice in academic test setting.

The right-hand sides in all tests are specified as

$$\begin{aligned} \mathbf{f} &= -\operatorname{div}(\boldsymbol{\epsilon}(\mathbf{u}_{\text{ex}}) + \lambda \operatorname{div} \mathbf{u}_{\text{ex}} I) + \nabla p_{\text{ex}} \\ g &= -\operatorname{div} \mathbf{u}_{\text{ex}} + \tau K_0 \Delta p_{\text{ex}} - S p_{\text{ex}} \end{aligned}$$

where

$$p_{\text{ex}} = \phi(x, y) - \frac{1}{|\Omega|} \int_{\Omega} \phi(x, y) dx dy \in L_2^0(\Omega), \quad \mathbf{u}_{\text{ex}} = 0.01 \left( \frac{\partial \phi}{\partial y}, \frac{\partial \phi}{\partial x} \right)$$

and

$$\phi = (\sin(2\pi x) \sin(2\pi y))^2.$$

Following the theoretical findings, the employed stabilization parameter  $L$  in the fixed-stress iteration is

$$L := L^* = \frac{1}{\lambda + 1/2}, \quad (30)$$

see also Remark 5, unless specified explicitly otherwise.

The numerical tests are performed on meshes with mesh parameter  $h$  where all meshes are derived via uniform refinement of the coarse mesh given on the left of Fig. 1 for which  $h = 1/16$ .

On the right of Fig. 1 we have plotted the solid displacement  $\mathbf{u}$  which has been computed for the linear model for the choice of parameters  $h = 1/32$ ,  $\tau = 0.01$ ,  $S = 10^{-4}$ ,  $K_0 = 10^{-6}$ , and  $\lambda = 10^2$ . The corresponding  $p$  has been shown on the left of Fig. 2, whereas on the right of the same figure we have presented the solution of the non-linear problem (i) for the same choice of parameters where additionally we have set  $K_1 = 10^{-1}$ .

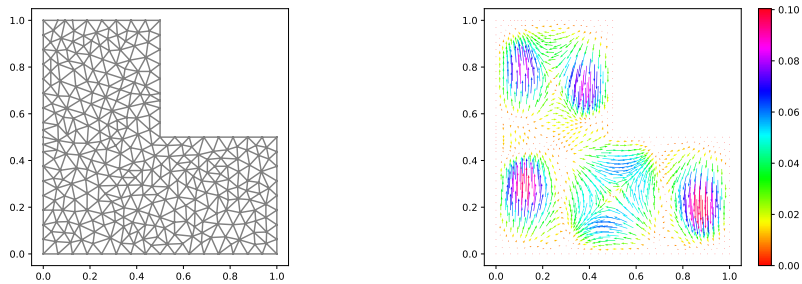


**Fig. 1:** Left - triangulation of  $\Omega$ ,  $h = 1/16$ , right -  $u$  for model (o), where  $h = 1/32$ ,  $\tau = 0.01$ ,  $S = 10^{-4}$ ,  $K_0 = 10^{-6}$  and  $\lambda = 10^2$ .

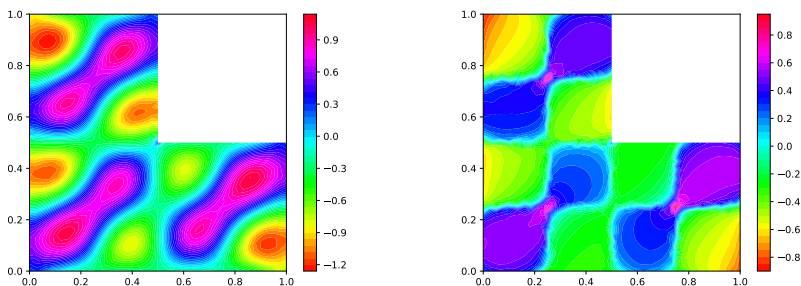


**Fig. 2:** Left -  $p$  for model (o), right -  $p$  for model (i). For both  $h = 1/32$ ,  $\tau = 0.01$ ,  $S = 10^{-4}$ ,  $K_0 = 10^{-6}$  and  $\lambda = 10^2$ , additionally for the non-linear model we have set  $K_1 = 10^{-1}$ .

To ascertain the robustness of the proposed fixed-stress method we vary the involved model, discretization and stabilization parameters. In all test settings we have tried to capture the most interesting ranges of the latter and to challenge the theoretical results.

The stopping criterion for the fixed-stress algorithm has been chosen to be

$$\|x_{k+1} - x_k\| < 10^{-6}, \quad (31)$$

where  $x_k$  denotes the  $k$ -th iterate of the proposed fixed-stress method.

The numerical experiments have been performed using the FEniCS open-source computing platform for solving partial differential equations, [53, 54].

## 4.1 Test setting (o)

In the focus of the first group of experiments is the linear model. The main purpose of these tests is to determine how the proposed fixed-stress method behaves in terms of number of fixed stress iterations when varying the model parameters and later compare with the results obtained for the non-linear models.

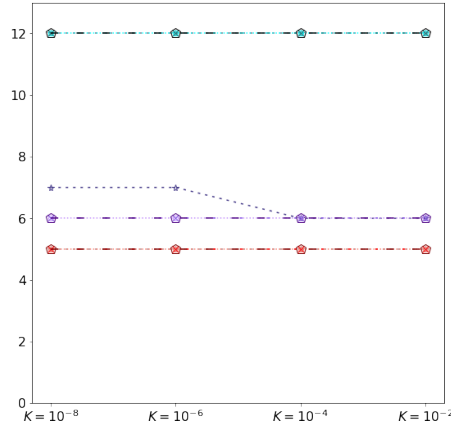


**Fig. 3:** Number of fixed-stress iterations for the linear model where we have set  $\tau = 0.01$ ,  $S = 10^{-4}$  and  $h \in \{1/16, 1/32, 1/64, 1/128\}$ . Blue range of colors -  $\lambda = 10^1$ , violet range of colors -  $\lambda = 10^2$  (single dotted line for  $h = 1/16$ ), red range of colors -  $\lambda = 10^3$ .

As can be seen from Fig. 3, the method shows robust behaviour in all tested parameter regimes.

## 4.2 Test setting (i)

Subject of testing in this subsection is the Biot model with non-linear permeability coefficient  $K(\operatorname{div} \mathbf{u}) = K_0 + K_1(\operatorname{div} \mathbf{u})^2$ .

On Fig. 4 the number of fixed-stress iterations are plotted for different model and discretization parameters where two different stopping criteria have been considered. The first is as defined in (31) and the second one is a residual reduction by factor  $10^6$ , i.e.,

$$\frac{\|r_k\|}{\|r_0\|} < 10^{-6},$$

where  $r_k$  denotes the  $k$ -th residual of the fixed-stress scheme. We observe that the number of iterations when using the second stopping criterion is always smaller and, furthermore, that this number is independent of the considered discretization and model parameters. Though slightly varying, the number of iterations when using the stopping criterion (31) also show the robustness of the studied iterative method.

For this choice of permeability we have additionally performed a series of tests where we have primarily varied  $\tau$ . It is interesting to observe on Fig. 5 that though

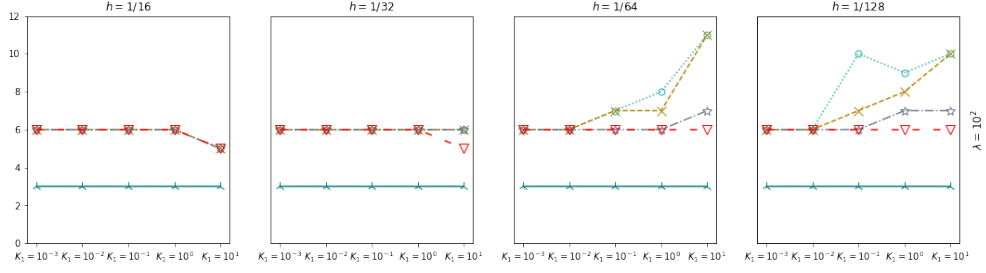


**Fig. 4:** Number of fixed-stress iterations for  $K = K_0 + K_1(\text{div } \mathbf{u})^2$ ,  $S = 10^{-4}$  where we have set  $\tau = 0.01$ ,  $S = 10^{-4}$  and  $\lambda = 10^2$ . Red line -  $K_0 = 10^{-8}$ , gray line -  $K_0 = 10^{-6}$ , yellow line -  $K_0 = 10^{-4}$ , blue line -  $K_0 = 10^{-2}$ . The blue-green line shows the results for a different stopping criterion, namely a residual reduction by factor  $10^6$ , which are identical for the four different choices of  $K_0$ .

for bigger  $\tau$  we have the smallest number of iterations when solving on the coarser meshes, on the finest mesh the algorithm converges only for the two smallest choices of  $\tau$ . This artefact, however, is in accordance with the analysis presented in this paper suggesting that for smaller mesh parameter  $h$  we might need a smaller time-step  $\tau$  to guarantee the convergence of the fixed-stress split method.

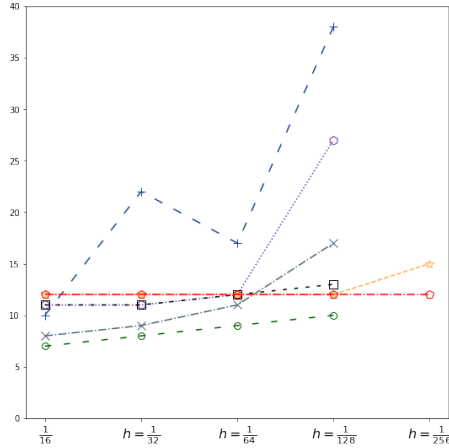


**Fig. 5:** Number of fixed-stress iterations for  $K = K_0 + K_1(\text{div } \mathbf{u})^2$ . Red line -  $\tau = 0.0001$ , orange line -  $\tau = 0.0005$ , black line -  $\tau = 0.001$ , violet line -  $\tau = 0.005$ , blue line -  $\tau = 0.01$ , grey line -  $\tau = 0.05$ , green line -  $\tau = 0.1$ . Missing points means that the algorithm does not converge for the corresponding parameter values.

### 4.3 Test setting (ii)

In this subsection we want to test the effect of the stabilization parameter  $L$  on the convergence of the considered iterative scheme. The studied model here involves the non-linear permeability  $K(\operatorname{div} \mathbf{u}) = (K_0 + K_1 \operatorname{div} \mathbf{u})^2$ .

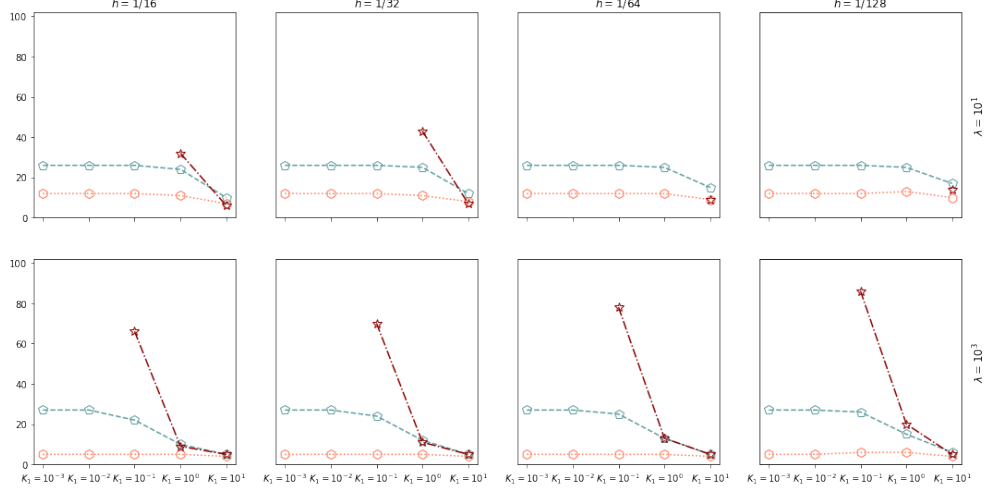


**Fig. 6:** Number of fixed-stress iterations for  $K = K(\operatorname{div} \mathbf{u}) = (K_0 + K_1 \operatorname{div} \mathbf{u})^2$ . We have set  $\tau = 0.01$  and  $S = 10^{-4}$ . Pink line - stabilization parameter  $L = L^*$  as in (30), blue line  $L = 2L^*$ , red line  $L = L^*/2$ . Missing points means no convergence within 100 iterations.

The results in Fig. 6 demonstrate the expected robust convergent behavior of the method for  $L = L^*$ , chosen as in (30), as well as for  $L = 2L^*$ , which is in accordance with the developed theory. Moreover, when  $L$  is too small, as in the example when  $L = L^*/2$ , we observe that the algorithm indeed does not converge in some parameter regimes. The tests indicate also that the method performs better when  $L$  is smaller but satisfies the theoretical bounds.

### 4.4 Test setting (iii)

In our last setting we tested the algorithm for a wide range of model and discretization parameters when  $K = K_0 e^{K_1 \operatorname{div} \mathbf{u}}$ . As can be seen from Fig. 7, the method shows robust behavior with respect to varying all parameters.

## 5 Conclusions

In this paper we have developed a new fixed-stress split method for a nonlinear poroelasticity model in which the permeability depends on the divergence of the



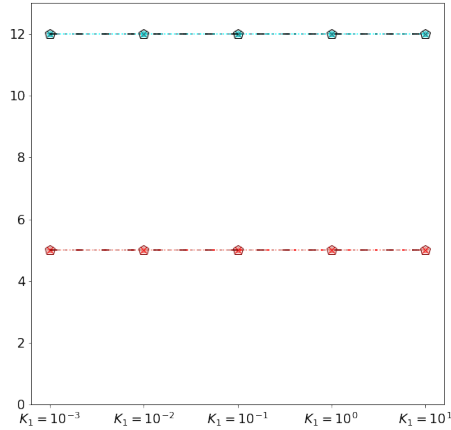


**Fig. 7:** Number of fixed-stress iterations for  $K = K_0 e^{K_1 \text{div } \mathbf{u}}$ ,  $S = 10^{-4}$ ,  $K_0 \in \{10^{-8}, 10^{-6}, 10^{-4}, 10^{-2}\}$ ,  $h \in \{1/16, 1/32, 1/64, 1/128\}$ . Blue range of colors -  $\lambda = 10^1$ , red range of colors -  $\lambda = 10^3$ .

displacement. We have proven that for sufficiently small time steps this algorithm converges linearly and the error contraction factor is strictly less than one, independently of all model parameters.

Moreover, our theoretical findings are fully supported and justified by a series of numerical tests which also have shown the robustness and computational efficiency of the proposed fixed-stress method.

## Acknowledgements

JK acknowledges the funding by the German Science Fund (DFG) - project “Physics-oriented solvers for multicompartamental poromechanics” under grant number 456235063. FAR acknowledges the support of the VISTA program, The Norwegian Academy of Science and Letters and Equinor.

## References

- [1] Detournay, E., Cheng, A.H.-D.: Fundamentals of poroelasticity. In: Analysis and Design Methods, pp. 113–171. Elsevier, ??? (1993)
- [2] Detournay, E., Cheng, A.-D.: Poroelastic response of a borehole in non-hydrostatic stress field. *Int. J. Rock Mech. Mining Sci.* **25**(25), 171–182 (1988)
- [3] Jha, B., Juanes, R.: Coupled multiphase flow and poromechanics: A computational model of pore pressure effects on fault slip and earthquake triggering. *Water Resources Research* **50**(5), 3776–3808 (2014)
- [4] Cowin, S.C.: Bone poroelasticity. *Journal of biomechanics* **32**(3), 217–238 (1999)

- [5] Roose, T., Netti, P.A., Munn, L.L., Boucher, Y., Jain, R.K.: Solid stress generated by spheroid growth estimated using a linear poroelasticity model. *Microvascular research* **66**(3), 204–212 (2003)
- [6] Carter, D.R., Wong, M.: Modelling cartilage mechanobiology. *Philosophical Transactions of the Royal Society of London. Series B: Biological Sciences* **358**(1437), 1461–1471 (2003)
- [7] Konofagou, E.E., Harrigan, T.P., Ophir, J., Krouskop, T.A.: Poroelastography: imaging the poroelastic properties of tissues. *Ultrasound in medicine & biology* **27**(10), 1387–1397 (2001)
- [8] Kyriacou, S.K., Mohamed, A., Miller, K., Neff, S.: Brain mechanics for neurosurgery: modeling issues. *Biomechanics and modeling in mechanobiology* **1**(2), 151–164 (2002)
- [9] Bohr, T., Hjorth, P.G., Holst, S.C., Hrabětová, S., Kiviniemi, V., Lilius, T., Lundgaard, I., Mardal, K.-A., Martens, E.A., Mori, Y., et al.: The glymphatic system: Current understanding and modeling. *Iscience* **25**(9) (2022)
- [10] Terzaghi, K., Peck, R.B., Mesri, G.: *Soil mechanics in engineering practice* (1996)
- [11] Biot, M.A.: General theory of three-dimensional consolidation. *Journal of applied physics* **12**(2), 155–164 (1941)
- [12] Biot, M.A.: Theory of elasticity and consolidation for a porous anisotropic solid. *Journal of applied physics* **26**, 182–185 (195)
- [13] Coussy, O.: *Mechanics of porous continua*. Wiley, West Sussex (1995)
- [14] Showalter, R.E.: Diffusion in poro-elastic media. *J. Math. Anal. Appl.* **251**(1), 310–340 (2000)
- [15] Showalter, R.E., Stefanelli, U.: Diffusion in poro-plastic media. *Math. Methods Appl. Sci.* **27**(18), 2131–2151 (2004)
- [16] Mikelić, A., Wheeler, M.F.: Theory of the dynamic Biot-Allard equations and their link to the quasi-static Biot system. *J. Math. Phys.* **53**(12), 123702–15 (2012)
- [17] Hiltunen, K.: *Mathematical and numerical modelling of consolidation processes in paper machines*. Jyväskylän Yliopisto (1995)
- [18] Raghavan, R., Chin, L.Y.: Productivity changes in reservoirs with stress-dependent permeability. In: *SPE Annual Technical Conference and Exhibition*, p. 77535 (2002)
- [19] Chin, L., Raghavan, R., Thomas, L.: Fully coupled geomechanics and fluid-flow

- analysis of wells with stress-dependent permeability. *Spe Journal* **5**(01), 32–45 (2000)
- [20] Barbeiro, S., Wheeler, M.F.: A priori error estimates for the numerical solution of a coupled geomechanics and reservoir flow model with stress-dependent permeability. *Computational Geosciences* **14**, 755–768 (2010)
- [21] Cao, Y., Chen, S., Meir, A.: Analysis and numerical approximations of equations of nonlinear poroelasticity. *Discrete & Continuous Dynamical Systems-Series B* **18**(5) (2013)
- [22] Cao, Y., Chen, S., Meir, A.: Steady flow in a deformable porous medium. *Mathematical Methods in the Applied Sciences* **37**(7), 1029–1041 (2014)
- [23] Cao, Y., Chen, S., Meir, A.: Quasilinear poroelasticity: Analysis and hybrid finite element approximation. *Numerical Methods for Partial Differential Equations* **31**(4), 1174–1189 (2015)
- [24] Bociu, L., Guidoboni, G., Sacco, R., Webster, J.T.: Analysis of nonlinear poro-elastic and poro-visco-elastic models. *Archive for Rational Mechanics and Analysis* **222**, 1445–1519 (2016)
- [25] Duijn, C., Mikelić, A.: Mathematical theory of nonlinear single-phase poroelasticity. *Journal of Nonlinear Science* **33**(3), 44 (2023)
- [26] Borregales, M., Radu, F.A., Kumar, K., Nordbotten, J.M.: Robust iterative schemes for non-linear poromechanics. *Computational Geosciences* **22**, 1021–1038 (2018)
- [27] Borregales, M., Kumar, K., Radu, F.A., Rodrigo, C., Gaspar, F.J.: A partially parallel-in-time fixed-stress splitting method for biot’s consolidation model. *Computers & Mathematics with Applications* **77**(6), 1466–1478 (2019)
- [28] Borregales Reverón, M.A., Kumar, K., Nordbotten, J.M., Radu, F.A.: Iterative solvers for biot model under small and large deformations. *Computational Geosciences* **25**, 687–699 (2021)
- [29] Kumar, K., Almani, T., Singh, G., Wheeler, M.F.: Multirate undrained splitting for coupled flow and geomechanics in porous media. In: *Numerical Mathematics and Advanced Applications—ENUMATH 2015*. *Lect. Notes Comput. Sci. Eng.*, vol. 112, pp. 431–440. Springer, ??? (2016)
- [30] Almani, T., Kumar, K., Dogru, A., Singh, G., Wheeler, M.F.: Convergence analysis of multirate fixed-stress split iterative schemes for coupling flow with geomechanics. *Comput. Methods Appl. Mech. Engrg.* **311**, 180–207 (2016)

- [31] Allen, D.R.: Stability, accuracy, and efficiency of sequential methods for coupled flow and geomechanics. Technical Report SPE119084, The SPE Reservoir Simulation Symposium, Houston, Texas (2009)
- [32] White, J.A., Castelletto, N., Tchelepi, H.A.: Block-partitioned solvers for coupled poromechanics: a unified framework. *Comput. Methods Appl. Mech. Engrg.* **303**, 55–74 (2016)
- [33] Castelletto, N., White, J.A., Ferronato, M.: Scalable algorithms for three-field mixed finite element coupled poromechanics. *J. Comput. Phys.* **327**, 894–918 (2016)
- [34] Gaspar, F.J., Rodrigo, C.: On the fixed-stress split scheme as smoother in multi-grid methods for coupling flow and geomechanics. *Comput. Methods Appl. Mech. Engrg.* **326**, 526–540 (2017)
- [35] Hong, Q., Kraus, J., Lymbery, M., Philo, F.: Conservative discretizations and parameter-robust preconditioners for biot and multiple-network flux-based poroelasticity models. *Numerical Linear Algebra with Applications* **26**(4), 2242 (2019)
- [36] Lee, J.J., Mardal, K.-A., Winther, R.: Parameter-robust discretization and preconditioning of Biot’s consolidation model. *SIAM J. Sci. Comput.* **39**(1), 1–24 (2017)
- [37] Hong, Q., Kraus, J.: Parameter-robust stability of classical three-field formulation of biot’s consolidation model. *ETNA - Electronic Transactions on Numerical Analysis* **48**, 202–226 (2018)
- [38] Hong, Q., Kraus, J., Lymbery, M., Wheeler, M.F.: Parameter-robust convergence analysis of fixed-stress split iterative method for multiple-permeability poroelasticity systems. *Multiscale modeling & simulation* **18**(2), 916–941 (2020)
- [39] Hong, Q., Kraus, J., Lymbery, M., Philo, F.: Parameter-robust Uzawa-type iterative methods for double saddle point problems arising in Biot’s consolidation and multiple-network poroelasticity models. *Math. Models Methods Appl. Sci.* **30**(13), 2523–2555 (2020)
- [40] Settari, A., Mourits, F.M.: A coupled reservoir and geomechanical simulation system. *SPE J.* **3**(3), 219–226 (1998)
- [41] Both, J.W., Kumar, K., Nordbotten, J.M., Radu, F.A.: The gradient flow structures of thermo-poro-visco-elastic processes in porous media. arXiv preprint arXiv:1907.03134 (2019)
- [42] Kim, J., Tchelepi, H.A., Juanes, R.: Stability and convergence of sequential methods for coupled flow and geomechanics: fixed-stress and fixed-strain splits.

- Comput. Methods Appl. Mech. Engrg. **200**(13-16), 1591–1606 (2011)
- [43] Kim, J., Tchelepi, H.A., Juanes, R.: Stability and convergence of sequential methods for coupled flow and geomechanics: drained and undrained splits. *Comput. Methods Appl. Mech. Engrg.* **200**(23-24), 2094–2116 (2011)
- [44] Almani, T., Manea, A., Kumar, K., Dogru., A.H.: Convergence of the undrained split iterative scheme for coupling flow with geomechanics in heterogeneous poroelastic media. *Computational Geosciences* **24**, 551–569 (2020)
- [45] Both, J.W., Borregales, M., Nordbotten, J.M., Kumar, K., Radu, F.A.: Robust fixed stress splitting for biot’s equations in heterogeneous media. *Applied Mathematics Letters* **68**, 101–108 (2017)
- [46] Almani, T., Kumar, K., Wheeler, M.F.: Convergence and error analysis of fully discrete iterative coupling schemes for coupling flow with geomechanics. *Comput. Geosci.* **21**(5-6), 1157–1172 (2017)
- [47] Mikelić, A., Wheeler, M.F.: Convergence of iterative coupling for coupled flow and geomechanics. *Comput. Geosci.* **17**(3), 455–461 (2013)
- [48] Both, J.W., Borregales, M., Nordbotten, J.M., Kumar, K., Radu, F.A.: Robust fixed stress splitting for Biot’s equations in heterogeneous media. *Applied Mathematics Letters* **68**, 101–108 (2017)
- [49] Storvik, E., Both, J.W., Kumar, K., Nordbotten, J.M., Radu, F.A.: On the optimization of the fixed-stress splitting for biot’s equations. *International Journal for Numerical Methods in Engineering* **120**(2), 179–194 (2019)
- [50] List, F., Radu, F.A.: A study on iterative methods for solving Richards’ equation. *Computational Geosciences* **20**(2), 341–353 (2016)
- [51] Both, J.W., Kumar, K., Nordbotten, J.M., Radu, F.A.: Anderson accelerated fixed-stress splitting schemes for consolidation of unsaturated porous media. *Computers & Mathematics with Applications* **77**(6), 1479–1502 (2019)
- [52] Hong, Q., Kraus, J., Lymbery, M., Wheeler, M.F.: Parameter-robust convergence analysis of fixed-stress split iterative method for multiple-permeability poroelasticity systems. *Multiscale Model. Simul.* **18**(2), 916–941 (2020)
- [53] Alnæs, M.S., Blechta, J., Hake, J., Johansson, A., Kehlet, B., Logg, A., Richardson, C., Ring, J., Rognes, M.E., Wells, G.N.: The fenics project version 1.5. *Archive of Numerical Software* **3**(100) (2015)
- [54] Logg, A., et al.: *Automated solution of differential equations by the finite element method.* Springer (2012)